



Contents lists available at ScienceDirect

Earth and Planetary Science Letters

journal homepage: www.elsevier.com/locate/epsl

Stable isotope analysis of the Cretaceous sulfur cycle

Alexandra V. Turchyn^{a,*}, Daniel P. Schrag^b, Rodolfo Coccioni^c, Alessandro Montanari^d^a Department of Earth Sciences, University of Cambridge, Cambridge, UK^b Department of Earth and Planetary Sciences, Harvard University, Cambridge MA, USA^c Dipartimento di Scienze dell'Uomo, dell'Ambiente e della Natura, Università degli Studi "Carlo Bo", Urbino, Italy^d Osservatorio Geologico di Coldigioco, Airolo, Italy

ARTICLE INFO

Article history:

Received 13 November 2008

Received in revised form 26 May 2009

Accepted 1 June 2009

Available online xxx

Editor: M.L. Delaney

Keywords:

barite

CAS

sulfur

oxygen

isotope

Cretaceous

ABSTRACT

We report the sulfur and oxygen isotope composition of sulfate ($\delta^{34}\text{S}_{\text{SO}_4}$ and $\delta^{18}\text{O}_{\text{SO}_4}$, respectively) in coexisting barite and carbonate-associated sulfate (CAS), which we use to explore temporal variability in the marine sulfur cycle through the middle Cretaceous. The $\delta^{34}\text{S}_{\text{SO}_4}$ of marine barite tracks previously reported sulfur isotope data from the tropical Pacific. The $\delta^{18}\text{O}_{\text{SO}_4}$ of marine barite exhibits more rapid and larger isotopic excursions than the $\delta^{34}\text{S}_{\text{SO}_4}$ of marine barite; these excursions temporally coincide with Ocean Anoxic Events (OAEs). Neither the $\delta^{34}\text{S}_{\text{SO}_4}$ nor the $\delta^{18}\text{O}_{\text{SO}_4}$ measured in marine barite resembles the $\delta^{34}\text{S}_{\text{SO}_4}$ or the $\delta^{18}\text{O}_{\text{SO}_4}$ measured in coexisting CAS. Culling our data set for elemental parameters suggestive of carbonate recrystallization (low [Sr] and high Mn/Sr) improves our record of $\delta^{18}\text{O}_{\text{SO}_4}$ in CAS in the Cretaceous. This suggests that the CAS proxy can be impacted by carbonate recrystallization in some marine sediments. A box model is used to explore the response of the $\delta^{34}\text{S}_{\text{SO}_4}$ and $\delta^{18}\text{O}_{\text{SO}_4}$ to different perturbations in the marine biogeochemical sulfur cycle. We conclude that the $\delta^{34}\text{S}_{\text{SO}_4}$ in the middle Cretaceous is likely responding to a change in the isotopic composition of pyrite being buried, coupled possibly with a change in riverine input. On the other hand, the $\delta^{18}\text{O}_{\text{SO}_4}$ is likely responding to rapid changes in the reoxidation pathway of sulfide, which we suggest may be due to anoxic versus euxinic conditions during different OAEs.

© 2009 Elsevier B.V. All rights reserved.

1. Introduction

Reconstructing temporal variability in the sulfur cycle remains an important paleoceanographic goal (e.g. [Petsch and Berner, 1996](#); [Berner, 2004](#)). The marine carbon and sulfur cycles are linked through bacterial sulfate reduction in organic-rich sediments, which is responsible for the remineralization of the majority of buried organic matter ([Kasten and Jørgensen, 2000](#)). Understanding precisely how the marine biogeochemical carbon and sulfur cycles respond to one another, however, remains largely unresolved. For example, in the Cretaceous (145.5 to 65.5 Ma) several lines of evidence suggest sulfate concentrations 60 to 80% lower than today (e.g. fluid inclusions – [Horita et al., 2002](#); [Lowenstein et al., 2001](#), and major ion modeling – [Berner, 2004](#)), which by first principles could imply more organic matter burial, impacting both the carbon cycle and atmospheric oxygen ([Berner, 2004](#); [Falkowski et al., 2005](#)). The Cretaceous was also a period of extreme carbon cycle instability, when the oceans periodically went anoxic during “Ocean Anoxic Events” (OAEs) (e.g. [Jenkyns, 1980](#); [Arthur et al., 1985, 1990](#)). How observations of low

sulfate concentrations and carbon cycle variability are linked – if at all – remains ambiguous.

The measurement of both the sulfur and oxygen isotopic composition ($\delta^{34}\text{S}_{\text{SO}_4}$ and $\delta^{18}\text{O}_{\text{SO}_4}$, respectively) of sulfate minerals can be a powerful tool for reconstructing the biogeochemical sulfur cycle. Temporal changes in the $\delta^{34}\text{S}_{\text{SO}_4}$ are driven by changes in the amount or isotopic composition of pyrite burial, river input, and hydrothermal circulation ([Paytan et al., 2004](#); [Berner, 2004](#)). Temporal changes in the $\delta^{18}\text{O}_{\text{SO}_4}$ of marine sulfate, on the other hand, are driven mainly by changes in the pathways by which sulfur is cycled between its oxidized and reduced states in organic-rich sediments ([Turchyn and Schrag, 2006](#)). Measuring both isotopes through time offers a more complete picture of temporal changes in the biogeochemical sulfur cycle.

When the $\delta^{34}\text{S}_{\text{SO}_4}$ and the $\delta^{18}\text{O}_{\text{SO}_4}$ measured in sulfate minerals do not covary, for example the sulfur cycle is likely responding to changes in pyrite burial or its isotopic composition, which affects the $\delta^{34}\text{S}_{\text{SO}_4}$, or changes in the pathways of sulfide reoxidation, which affects the $\delta^{18}\text{O}_{\text{SO}_4}$. For example, if a shift to lower values is recorded in the $\delta^{34}\text{S}_{\text{SO}_4}$ of sulfate minerals that is not accompanied by any change in the $\delta^{18}\text{O}_{\text{SO}_4}$ then the sulfur cycle cannot be responding to a sharp change in river input, such as increased pyrite weathering, because this should be manifest in the $\delta^{18}\text{O}_{\text{SO}_4}$ as well ([Turchyn and Schrag, 2006](#)). In this example, the $\delta^{34}\text{S}_{\text{SO}_4}$ could be responding to a change in the isotopic composition of pyrite or a decrease in the relative pyrite

* Corresponding author. University of Cambridge, Downing Street, Cambridge, CB2 3EQ UK. Tel.: +44 1223 333479.

E-mail address: avt25@cam.ac.uk (A.V. Turchyn).

burial, neither of which would necessarily impact the $\delta^{18}\text{O}_{\text{SO}_4}$. Because decoupled sulfur and oxygen isotope behavior specifically highlights changes in redox processes in organic-rich sediments, this dual isotope approach offers the greatest possibility to use changes in the sulfur cycle to help decipher changes in the carbon cycle.

The four most commonly used types of sulfate minerals available for both sulfur and oxygen isotope analysis are evaporite minerals (e.g. gypsum, $\text{CaSO}_4 \cdot 2(\text{H}_2\text{O})$), phosphate-bound sulfate, marine barite (barium sulfate – BaSO_4) and carbonate-associated-sulfate (CAS). Evaporite minerals and phosphate-bound sulfate are least favorable because they are often not temporally continuous or, in the case of phosphate-bound sulfate, require extensive phosphorite deposition (Claypool et al., 1980; Shields et al., 1999). For this study, we analyzed marine barite and CAS. Barite forms in the water column and is preserved in oxic, pelagic sediments where bacterial sulfate reduction is minimal (Bishop, 1988; Ganeshram et al., 2003). Because pelagic sediments are largely confined to the modern deep ocean, barite's use as a paleoceanographic proxy is typically limited to the last 150 million years (Paytan et al., 2004). CAS, on the other hand, forms with carbonate minerals; the sulfate ion is substituted for the carbonate ion in the mineral lattice and exists as a mineral defect (Burdett et al., 1989; Kampschulte and Strauss, 2004). The concentration of CAS in modern carbonates ranges from a few hundred to a few thousand ppm (Burdett et al., 1989). CAS is preserved where carbonate minerals and rocks are preserved, mainly in continental shelf settings. Using ancient carbonate platform sediments, CAS allows the reconstruction of the sulfur cycle much earlier in Earth history (e.g. Hurtgen et al., 2002; Kampschulte and Strauss, 2004; Hurtgen et al., 2006).

In theory, the $\delta^{34}\text{S}$ and $\delta^{18}\text{O}_{\text{SO}_4}$ of coexisting barite and CAS should be the same, provided they both form in equilibrium with seawater, unless one of three things has occurred: either the barite or the CAS has undergone diagenetic alteration and no longer has its original isotopic composition, or the minerals precipitated from isotopically distinct water masses (Burdett et al., 1989; Strauss, 1999). Although the two minerals are mainly preserved in contrasting environments, CAS should also be preserved in pelagic, carbonate-rich settings, allowing a direct comparison of barite and CAS in the same sample. The reverse is not true; the majority of barite extracted from continental shelves is diagenetic in nature (Torres et al., 1996; Paytan et al., 2002). In this paper we present analysis of both the sulfur and oxygen isotope composition of barite and CAS from pelagic sediments. We will first compare the isotope measurements made in the coexisting barite and CAS, then we will explore the isotope record in barite throughout the middle Cretaceous.

2. Methods

We extracted barite and CAS minerals from rocks and sediments collected in various pelagic environments in the Cretaceous. The majority of our data is generated from samples from the Umbria-Marche Apennines in central Italy; these sediments were originally deposited in the Tethys ocean. Sulfur isotope analysis was also performed on selected samples from DSDP Site 305 (in the North-west Pacific Ocean) and ODP Site 766 (in the Eastern Indian Ocean); these sites were chosen based on their previous success in extracting marine barite (Paytan et al., 2004). Samples within DSDP/ODP cores and Italian outcrop were selected for high carbonate and negligible organic matter content, maximizing the possibility that all sulfate minerals are primary (Moberly et al., 1975; Arthur and Fisher, 1977; Ludden et al., 1990). Our samples were not taken from any layers that had either visible pyrite or pyrite concretions, which could significantly affect our analyses.

Sediment was pulverized and digested in deionized water and then soaked in a sodium hypochlorite solution to oxidize any reduced sulfur compounds that might have been present. This

effluent was discarded. The remaining sediment was rinsed and digested in a 10% acetic acid solution at room temperature. The digestion was less than 1 hr, and the sulfate ions released from carbonate dissolution had minimal exposure to acid to ensure no isotope exchange with water could occur (Lloyd, 1968). The effluent was filtered and a 0.1 M barium chloride solution was added to precipitate the sulfate that had been released from the carbonate lattice during dissolution. The barite formed from this precipitation was rinsed in 6N HCl to dissolve any barium carbonate that may have formed along with the barite. This barite, called CAS, was set aside for isotopic analysis.

The remaining insoluble residue from the acetic acid digestion was dried and ground to powder and barite was extracted per the procedure detailed in Turchyn and Schrag (2006). Barite samples were examined for their purity on a Scanning Electron Microscope (SEM) with Energy dispersive X-ray capabilities (EDAX). We estimate that our marine barite samples were at least 90% pure. Splits of both CAS and barite were weighed and crushed in tin boats with V_2O_5 , and sent to the Stable Isotope Facility at the University of Indiana, Bloomington for sulfur isotope analysis. There, they were run through a combustion oven (Carlo Erba) coupled to a Delta Plus Mass spectrometer. Sulfur isotope ratios are expressed in parts per thousand or permil (‰) with the standard Canon Diablo Troilite (CDT). Analytical error is around 0.2‰ (2σ).

At the Laboratory for Geochemical Oceanography at Harvard University, CAS and barite samples were weighed and crushed in silver boats and pyrolyzed in a Temperature Conversion Element Analyzer (TC/EA) coupled by continuous flow to a Delta Plus Mass Spectrometer where the $\delta^{18}\text{O}_{\text{SO}_4}$ was measured as carbon monoxide (Turchyn and Schrag, 2006). A standard of a known isotopic composition (NBS 127) was run before and after samples, and the $\delta^{18}\text{O}_{\text{SO}_4}$ of the samples was corrected to an NBS 127 value of 9.3‰. Analytical error of this measurement technique for $\delta^{18}\text{O}_{\text{SO}_4}$, based on repeat analysis of NBS 127 is -0.4% (2σ). Samples for $\delta^{18}\text{O}_{\text{SO}_4}$ were run in quadruplicate, as sample volume allowed. We have reported our data as the average of these replicate analyses. The standard error of the replicate measurements of samples run varies from 0.03 to 0.88‰ (see Supporting Online Material) though the vast majority of samples ran with a standard error between 0.1 and 0.4‰.

Elemental analyses (Sr, Mn) were performed on a Jovin Yvon 46P ICP-AES mass spectrometer at Harvard University's Laboratory for Geochemical Oceanography. All samples were prepared by dissolving ~ 4 mg of carbonate powder in 2% nitric acid. SCP multielement standards were used for element-specific calibration at the beginning of each run. External error (1σ stdev) determined by repeat analysis was $<7\%$ for all elements. The $\delta^{13}\text{C}$ and $\delta^{18}\text{O}$ of the carbonates was measured via an Isocarb preparation device coupled to a VG Optima dual inlet mass spectrometer. Approximately 1-mg carbonate samples reacted in a phosphoric acid bath at 90 °C. The CO_2 generated was collected and analysed. The 1σ stdev for this analysis is better than 0.1‰.

3. Results

A detailed data table with all our sulfur and oxygen isotope analyses over the Cretaceous is provided in the supporting online material. In Fig. 1 we present a complete sulfur and sulfate oxygen isotope plot versus stratigraphic section and age. The data, from left to right, are the $\delta^{18}\text{O}_{\text{SO}_4}$ of marine barite, the $\delta^{34}\text{S}$ of marine barite, the $\delta^{18}\text{O}_{\text{SO}_4}$ of CAS, and the $\delta^{34}\text{S}$ of CAS. The two $\delta^{18}\text{O}_{\text{SO}_4}$ curves (marine barite and CAS) are comprised of only measurements on samples from outcrop in the Umbria-Marche Apennines. The two $\delta^{34}\text{S}$ curves, on the other hand, represent samples from the Umbria-Marche Apennines as well as samples from DSDP Site 305 and ODP Site 766. The line on both sulfur isotope curves is a running average of the previously reported Paytan et al. (2004) $\delta^{34}\text{S}$ curve for marine barite

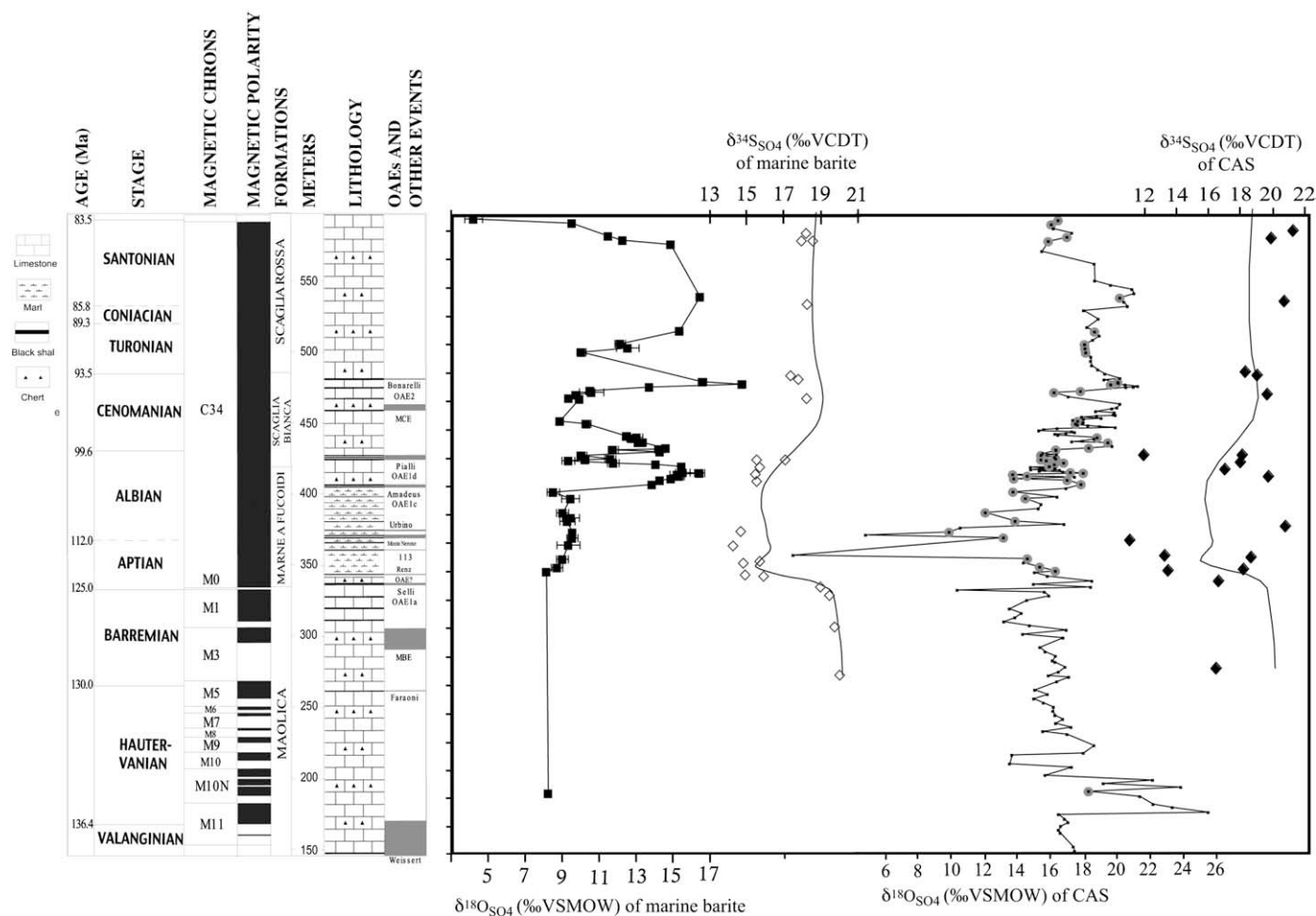


Fig. 1. A composite plot of sulfur and sulfate oxygen isotope in both barite and CAS versus stratigraphic height in the Umbria-Marche Apennines of Italy. The litho- and chronostratigraphy are according to Coccioni (1996), Sprovieri et al. (2006), and data from the Cretaceous Integrated Stratigraphy Project (CRIS) (coordinator R. Coccioni). The reported ages are from Gradstein et al. (2004). From left to right, the data are $\delta^{18}\text{O}_{\text{SO}_4}$ of marine barite (black squares), $\delta^{34}\text{S}$ of marine barite (open diamonds), $\delta^{18}\text{O}_{\text{SO}_4}$ of CAS (black curve with some gray circles), and $\delta^{34}\text{S}$ of CAS (black solid diamonds). The error bars on the $\delta^{18}\text{O}_{\text{SO}_4}$ of marine barite represent the standard error based on up to four replicate measurements. The points on the $\delta^{18}\text{O}_{\text{SO}_4}$ of CAS curve that are large gray circles represent samples where we have both barite and CAS $\delta^{18}\text{O}_{\text{SO}_4}$ data. The thin black line on both the $\delta^{34}\text{S}_{\text{SO}_4}$ of marine barite and the $\delta^{34}\text{S}_{\text{SO}_4}$ of CAS are the running average of the previously reported $\delta^{34}\text{S}_{\text{SO}_4}$ of marine barite by Paytan et al. (2004). All data except the $\delta^{18}\text{O}_{\text{SO}_4}$ of CAS are on the same scale. See text for details.

in the Cretaceous. Except for the $\delta^{18}\text{O}_{\text{SO}_4}$ of CAS, all the isotope plots are on the same scale. For every sample where there is a data point for $\delta^{18}\text{O}_{\text{SO}_4}$ of CAS, we attempted to recover marine barite from the insoluble residue. For the majority of these samples we were unsuccessful (55 out of 258 samples). This could be because there was no barite there or because it was too difficult to remove other dense minerals. CAS samples in Fig. 1 where the data point is a large gray circle represent samples where we were successfully able to subsequently extract marine barite.

Our $\delta^{34}\text{S}_{\text{SO}_4}$ in marine barite shows a 5‰ decrease from 120 to 115 Ma and a 4‰ increase from 95 to 90 Ma, reproducing the Paytan et al. (2004) data. The $\delta^{18}\text{O}_{\text{SO}_4}$ of marine barite exhibits large and rapid shifts of 5 to 7‰, which are not present in the sulfur isotope record (Fig. 1). These shifts coincide with OAEs (represented as the grey bars in Fig. 1). The $\delta^{18}\text{O}_{\text{SO}_4}$ remains constant across OAE1b, increases after OAE 1c, decreases after OAE 1d, and then increases both during the Mid-Cenomanian event (MCE) and OAE 2. The possible causes of this variable response will be discussed in detail below.

The $\delta^{34}\text{S}_{\text{SO}_4}$ of CAS is both isotopically heavier and lighter than the $\delta^{34}\text{S}_{\text{SO}_4}$ of the coexisting barite, and does not follow the previously published Paytan et al. (2004) curve (Fig. 1). In Fig. 2a, $\Delta^{34}\text{C}_{\text{barite-CAS}}$ is

plot versus time. Similarly, the $\delta^{18}\text{O}_{\text{SO}_4}$ of marine barite shows distinct shifts and temporal variability that are not resolved in the $\delta^{18}\text{O}_{\text{SO}_4}$ of CAS. The majority of $\delta^{18}\text{O}_{\text{SO}_4}$ of CAS data are isotopically lighter than the coexisting $\delta^{18}\text{O}_{\text{SO}_4}$ of barite (Fig. 2b – $\Delta^{18}\text{O}_{\text{barite-CAS}}$).

To ascertain the cause of the variability in the $\delta^{18}\text{O}_{\text{SO}_4}$ of CAS, we used elemental analysis on the bulk carbonate rocks from which the CAS was extracted to look for other signs of carbonate diagenesis. In Fig. 3 we present three crossplots, the $\delta^{18}\text{O}_{\text{SO}_4}$ of CAS versus the $\delta^{18}\text{O}$ of the carbonate mineral (Fig. 3a), versus the Mn/Sr (Fig. 3b), and versus Sr concentration (Fig. 3c). There is no correlation between the $\delta^{18}\text{O}_{\text{SO}_4}$ of CAS and the $\delta^{18}\text{O}$ of the carbonate minerals (Fig. 3a). When carbonate minerals recrystallize strontium is released and manganese is taken up, meaning low Sr concentrations or high Mn/Sr ratios can indicate recrystallized carbonates (Brand and Veizer, 1980). We cull our data here with Mn/Sr greater than 2 and [Sr] less than 300 ppm, similar to previous studies (e.g. Halverson et al., 2007). The replotted $\delta^{18}\text{O}_{\text{SO}_4}$ of CAS, along with the $\delta^{18}\text{O}_{\text{SO}_4}$ of barite is shown in Fig. 4. Much of the variability present particularly in the lower stratigraphic interval in the initial data set (Fig. 1) is no longer present and several of the shifts seen in the barite $\delta^{18}\text{O}_{\text{SO}_4}$ can now be resolved in the CAS $\delta^{18}\text{O}_{\text{SO}_4}$ although the absolute value of the $\delta^{18}\text{O}_{\text{SO}_4}$ between barite and CAS remains offset.

4. Discussion

4.1. CAS vs. barite record in the Cretaceous

The two sulfur mineral proxies, barite and CAS, from the environments we sampled do not measure the same sulfur or oxygen isotopic composition. There is no known isotope fractionation of either oxygen or sulfur isotopes into CAS based on modern measurements of core-tops and carbonate skeletons (Burdett et al., 1989; Lyons et al., 2004). There is also no sulfur isotope fractionation, but potentially a 1‰ oxygen isotope fractionation, during barite precipitation (Paytan et al., 1998; Turchyn and Schrag, 2004). It is unlikely that changes in isotope fractionation can explain the much larger differences between the $\delta^{18}\text{O}_{\text{SO}_4}$ of barite and CAS reported in this paper, and impossible for isotope fractionation to explain the difference in the $\delta^{34}\text{S}$ between barite and CAS.

Diagenetic barite forms in organic-carbon bearing sediments where sulfate reduction drives dissolution-reprecipitation of barite crystals. This altered barite is easily identified; the crystals are far larger, take on a “pitted” appearance in SEM images and have anomalously heavy sulfur isotopic composition (Torres et al., 1996; Paytan et al., 2002). As mentioned above, all of our barite samples were examined under an SEM to insure they had not undergone diagenetic alteration. Approximately 20 samples from the Cretaceous were discarded because they showed signs of barite diagenesis. We are confident that the discrepancy between the isotope composition of the barite and the CAS cannot be explained by diagenetic barite.

Identifying diagenetic CAS is more difficult. We define diagenetic CAS as that produced from carbonate recrystallization in sediments where, upon recrystallization, isotopically modified sulfate from the pore fluid is incorporated into the new carbonate lattice impacting the

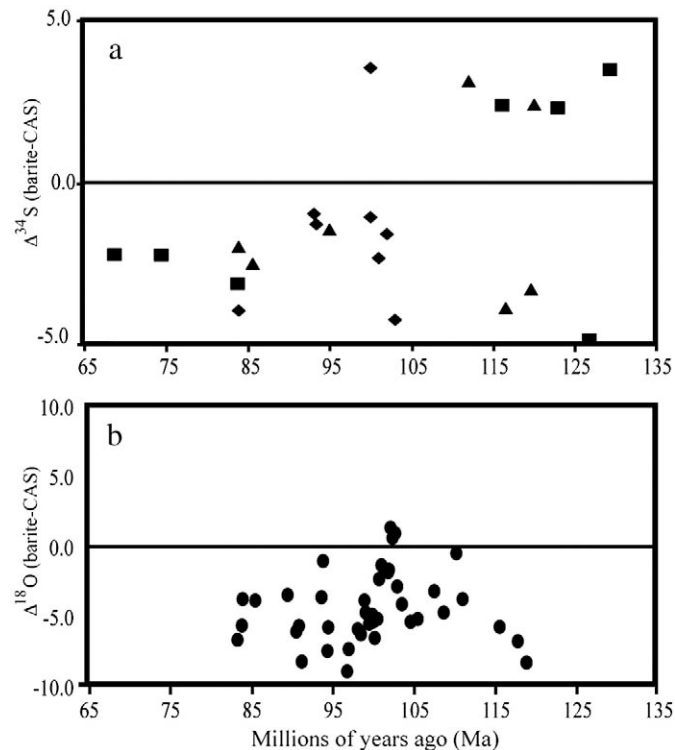


Fig. 2. 2a. $\Delta^{34}\text{S}(\text{barite-CAS})$ for our data. The square symbols represent samples from ODP Site 305, the triangles represent samples from ODP Site 766 (both also used by Paytan et al., 2004), and the diamonds represent samples from Cretaceous outcrop in the Umbria-Marche Apennines of Italy. 2b. $\Delta^{18}\text{O}(\text{barite-CAS})$. For both plots the points above the line represent samples where the barite is isotopically heavier than the CAS, the points below the line represent samples where the barite is isotopically lighter than the CAS.

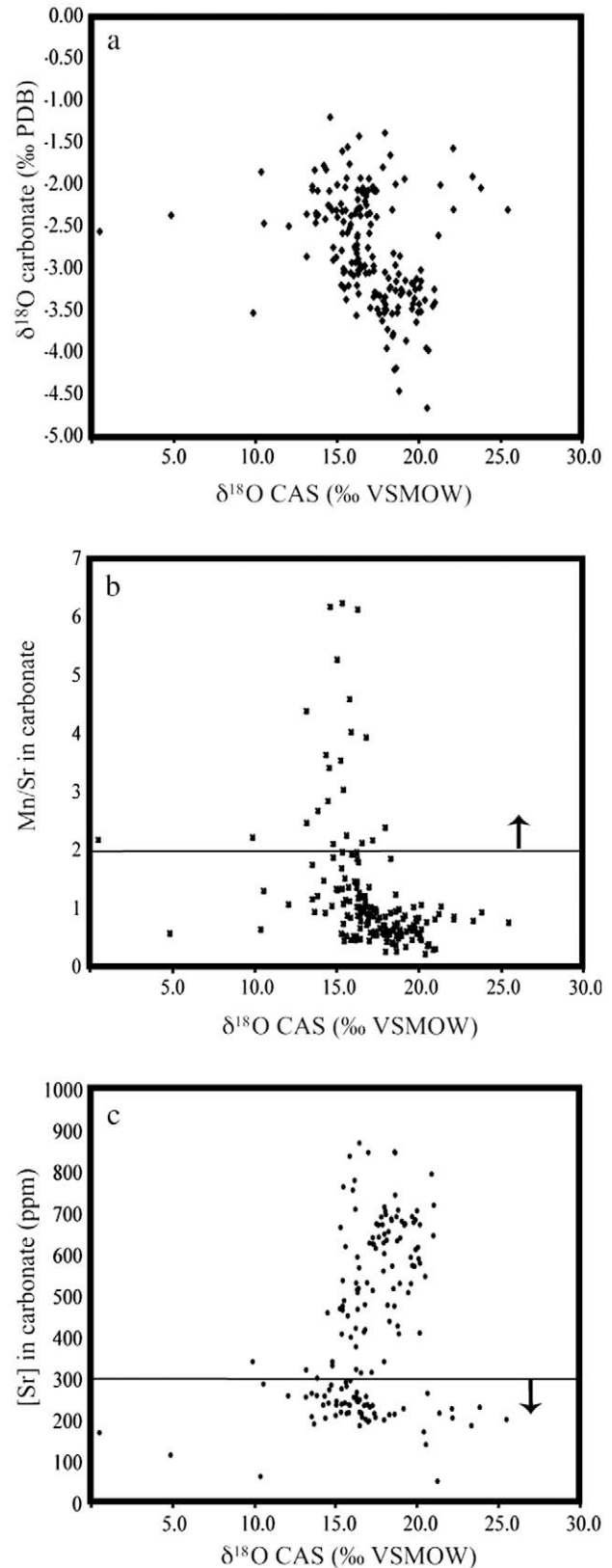


Fig. 3. Three crossplots of the $\delta^{18}\text{O}_{\text{SO}_4}$ of CAS versus the $\delta^{18}\text{O}$ of the carbonate (3a), Mn/Sr (3b) and [Sr] (3c). Lines on the plots indicate points above or below which the data was culled.

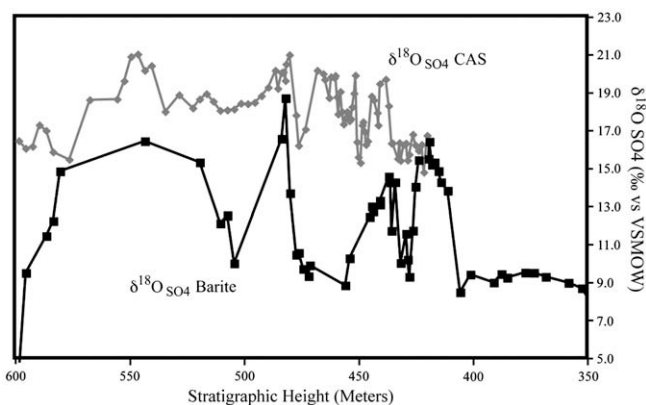


Fig. 4. Oxygen isotope data for barite and CAS replotted after CAS samples suspected of being affected by diagenetic recrystallization were removed (see Fig. 3). The CAS data is in gray and the barite data is in black. Both minerals $\delta^{18}\text{O}_{\text{SO}_4}$ are plotted on the same scale.

overall isotope composition of the CAS. Recent studies in the modern ocean have suggested that authigenic carbonate precipitation has little impact on the isotope composition of the incorporated sulfate (Lyons et al., 2004). These authors concluded that sulfate may not be incorporated into the carbonate lattice during diagenesis, or that the amount of authigenic carbonate is small compared to the seawater derived CAS and therefore CAS is largely buffered during carbonate recrystallization (Lyons et al., 2004).

Based on these results, we targeted specifically carbonate-rich organic-poor lithologies in this study. Unlike the Lyons et al. (2004) study, which focused on a shallow ocean setting, all our samples were originally deposited in pelagic, carbonate-rich settings, to ensure barite preservation. The nature of carbonate diagenesis in pelagic settings is different than in shallow platform or epicontinental seas; in pelagic settings, recrystallization can continue for hundreds of meters in the sediment, whereas on carbonate platforms lithification occurs within meters of the sediment-water interface (Morse and Mackenzie, 1990; Fantle and DePaolo, 2007; Walter et al., 2007). This suggests that shallow carbonate platforms may be better able to preserve a primary CAS isotope signal (Lyons et al., 2004). Indeed, high-resolution isotope analysis of CAS measured on late Neoproterozoic and Paleozoic carbonate platforms suggests that there are sections that must preserve a chemical signature of sulfur cycle variability (e.g. Hurtgen et al., 2006; Fike et al., 2006; Gill et al., 2007).

The possible modification of the CAS signal specifically in pelagic settings will depend on the isotopic composition of the pore fluid sulfate, the extent of recrystallization, and whether the recrystallized minerals incorporate pore fluid sulfate. Studies of the $\delta^{18}\text{O}_{\text{SO}_4}$ and $\delta^{34}\text{S}_{\text{SO}_4}$ of pore fluid sulfate have shown that even small amounts of sulfate reduction drive rapid increases in the residual sulfur and oxygen isotope composition of pore fluid sulfate (Wortmann et al., 2007). Thus it is easier to blame CAS diagenesis for the data points that lie below the line in Fig. 2a and b – that is samples where the CAS has been reset to isotopically heavier values through the incorporation of “heavy” pore fluid.

If the variability in our measured $\delta^{18}\text{O}_{\text{SO}_4}$ and $\delta^{34}\text{S}_{\text{SO}_4}$ measured in CAS is driven by diagenetic recrystallization, this underscores the need to understand depositional environment, for based on lithology alone, our samples would be excellent targets for CAS extraction and isotope analysis. It is somewhat comforting to find that when we cull our complete $\delta^{18}\text{O}_{\text{SO}_4}$ of CAS record for samples with low [Sr] and higher Mn/Sr ratios, some of the trends of the barite record become more apparent in the $\delta^{18}\text{O}_{\text{SO}_4}$ of CAS (Fig. 4). However, the minerals are not measuring the same absolute isotopic composition; this is not easily explained. The possibility remains that there could be isotopic fractionation in these mineral systems (CAS or barite) that is not fully understood.

One final possibility to explain our CAS data is that variations in the extraction technique can impart their own isotope signature on the analyzed CAS (e.g. Marengo et al., 2008). We oxidized our samples in bleach for up to 30 min and discarded the effluent in an attempt to remove any pyrite or organic sulfur from our samples. More recent work, however, has suggested that this oxidation step needs to be significantly longer, as much as 24 hr, to oxidize all possible reduced sulfur in sediments (e.g. Gill et al., 2007). The oxidation step is followed by a simple acid dissolution to release the sulfate from the carbonate lattice; however, some acids used can also oxidize pyrite (Marengo et al., 2008). This will create an ambiguous isotopic signal – with part of the signal derived from the CAS and part from the other sulfur contaminants. Since these contaminants are often “light” they could help explain the data points in Fig. 2a and b that are above the line – that is where the CAS is lighter than the coexisting barite. Further work is needed to understand the possible effects of both authigenic carbonate precipitation and variability in extraction techniques on the CAS isotope signal.

4.2. The paleoceanographic sulfur cycle

One of the outstanding questions about the Cretaceous is whether sulfate concentrations were significantly lower than today and how this might have impacted the biogeochemical sulfur and carbon cycles. Fluid inclusion data suggests that sulfate concentrations may have been as low as 8 to 12 mM, or 60–70% lower than the modern oceans. Our record of the $\delta^{34}\text{S}_{\text{SO}_4}$ and the $\delta^{18}\text{O}_{\text{SO}_4}$ through the Cretaceous (Fig. 1), particularly the rapid isotopic shifts observed in both isotope records, is also consistent with these low marine sulfate concentrations.

As shown in Fig. 1, the $\delta^{18}\text{O}_{\text{SO}_4}$ and the $\delta^{34}\text{S}_{\text{SO}_4}$ of marine barite are decoupled across the middle Cretaceous. This suggests that the $\delta^{18}\text{O}_{\text{SO}_4}$ must be responding to changes in the pathways of sulfide oxidation (Turchyn and Schrag, 2006). Our understanding of the various pathways of sulfide oxidation and their related oxygen isotope fractionation is still being developed. When sulfide oxidation is bacterially mediated in modern sediments, the $\delta^{18}\text{O}_{\text{SO}_4}$ of the resulting sulfate is typically anywhere from 10 to 20‰ isotopically heavier than the $\delta^{18}\text{O}$ of the water where it was oxidized (Van Stempvoort and Krouse, 1994). This strong oxygen isotope enrichment occurs because sulfur intermediates can equilibrate intercellularly with water and strongly enrich the product sulfate in ^{18}O . This pathway of sulfide oxidation is likely dominant where sulfide oxidizing bacteria thrive, in strongly anoxic sediments, using either nitrate or iron/manganese oxyhydroxides as electron acceptors (e.g. Van Stempvoort and Krouse, 1994). Abiotic sulfide oxidation, which could occur with the rapid mixing of sulfide-rich waters into oxygen-rich waters, is less well understood. Lab experiments suggest that the oxygen comes into the abiotically oxidized sulfate with minimal fractionation, producing sulfate with a $\delta^{18}\text{O}_{\text{SO}_4}$ that more closely resembles water (e.g. Lloyd, 1968; Turchyn and Schrag, 2004, 2006). One thought is that this pathway dominates in less anoxic sediments, where bioturbation rapidly returns sulfide to the well-oxygenated bottom ocean waters (Van Stempvoort and Krouse, 1994).

The impact of changes in the sulfide oxidation pathway on the $\delta^{18}\text{O}_{\text{SO}_4}$ recorded in marine barite has been explored over the Cenozoic, where the $\delta^{18}\text{O}_{\text{SO}_4}$ oscillates by 5 to 6‰, while the $\delta^{34}\text{S}_{\text{SO}_4}$ was essentially constant (Turchyn and Schrag, 2006). The interpretation of this dataset was that increases in the $\delta^{18}\text{O}_{\text{SO}_4}$ were due to more concentrated organic carbon burial (fewer sediments with higher percentages of organic carbon), producing more microbial sulfide oxidation and isotopically heavier $\delta^{18}\text{O}_{\text{SO}_4}$, and decreases were due to more diffuse organic carbon burial (more sediments with lower percentages of organic carbon), producing more abiotic sulfide oxidation and lighter $\delta^{18}\text{O}_{\text{SO}_4}$ (Turchyn and Schrag, 2006). This interpretation suggests that changing the types of sediments where

Table 1
Model scenario parameters.

Model Scenario	River Flux	$\delta^{18}\text{O}$ riv	$\delta^{18}\text{S}$ riv	Pyrite Flux	ϵS^a	% reoxidized	ϵO^b		
Initial conditions	3	5	13	1.3	14	90	12.6	A steady state ocean (10 mM sulfate, $\delta^{18}\text{O}_{\text{SO}_4} = 9\%$, $\delta^{34}\text{S} = 16\%$)	
1	Fig. 5a	3	5	13	2.3	14	90	12.6	Increased pyrite burial through increased sea level
2	Fig. 5b	3	5	13	1.3	23	90	12.6	Increased sulfur isotope fractionation creating isotopically lighter pyrite
3	Fig. 5c	3	5	13	2.5	14	70	12.6	Increased pyrite burial through decreased reoxidation
4	Fig. 5d	4	10	16	1.3	14	90	12.6	Increased river weathering of evaporites
5	Fig. 5e	3	5	13	1.3	14	90	18	Increased oxygen isotope fractionation during sulfide reoxidation

Fluxes are in 10^{12} mol S/year, isotopes are in ‰. The first line of the table has the arrangement of model parameters for a steady state ocean with 10 mM sulfate, 9‰ $\delta^{18}\text{O}_{\text{SO}_4}$ and 16‰ $\delta^{34}\text{S}$ (these numbers are in bold). The parameter in each subsequent line correspond to the model runs in the text (in italics). The parameter that was changed in each model run is indicated in bold and italics.

^a Isotopic fractionation during sulfate reduction – determining the sulfur isotope composition of pyrite.

^b Isotopic fractionation during sulfide reoxidation – determining the average oxygen isotope composition of the reoxidized flux.

organic carbon is buried can have a substantial impact on the pathways by which sulfur is cycled and marine $\delta^{18}\text{O}_{\text{SO}_4}$, although these changes may not change the overall global rate of pyrite burial or its isotopic composition, and thus may not affect marine $\delta^{34}\text{S}_{\text{SO}_4}$.

We now report similar decoupling of the $\delta^{34}\text{S}_{\text{SO}_4}$ and the $\delta^{18}\text{O}_{\text{SO}_4}$ in the middle Cretaceous. This is more complicated than in the Cenozoic because the $\delta^{34}\text{S}_{\text{SO}_4}$ does vary but in a different manner and magnitude than the $\delta^{18}\text{O}_{\text{SO}_4}$. An additional complication is the fact that the $\delta^{34}\text{S}_{\text{SO}_4}$ and the $\delta^{18}\text{O}_{\text{SO}_4}$ have different response times; in the modern ocean sulfur isotopes in marine sulfate have a residence time of 10 to 20 million years whereas oxygen isotopes in marine sulfate have a residence time closer to 1 million years.

To explore the possible causes of decoupled sulfur and oxygen isotope behavior in the Cretaceous, we use the basic box model first introduced in Turchyn and Schrag (2004), and elaborated in Turchyn and Schrag (2006). To summarize, three coupled conservation equations describe a simple one-box model of marine sulfate and its sulfur and oxygen isotopic composition. Sulfate concentrations vary as a function of changes in river input, pyrite burial, and burial as evaporites and in hydrothermal systems. Pyrite burial is the difference between the global sulfate reduction rate (a function of shelf area) and the percentage of sulfide reoxidized globally (assigned). In separate equations each flux is assigned a sulfur and oxygen isotope composition. The conservation equations are coupled through the burial term and the sulfate reduction rate term, which are functions of the amount of sulfate in the ocean, allowing us to simultaneously model $\delta^{18}\text{O}_{\text{SO}_4}$, $\delta^{34}\text{S}_{\text{SO}_4}$, and marine sulfate concentrations.

We begin our model in steady state with marine sulfate concentrations of 10 mM and $\delta^{18}\text{O}_{\text{SO}_4}$ of 9‰ and $\delta^{34}\text{S}_{\text{SO}_4}$ of 16‰. In each scenario, we run the model for 20 million years in 10,000 year time steps, and 3 million years into each model run we change one parameter to see how the $\delta^{34}\text{S}_{\text{SO}_4}$ and $\delta^{18}\text{O}_{\text{SO}_4}$ variably respond. We run five model scenarios, which are summarized in Table 1 and $\delta^{18}\text{O}_{\text{SO}_4}$, $\delta^{34}\text{S}_{\text{SO}_4}$, sulfate concentrations, and pyrite burial rates for each model scenario are presented in Fig. 5.

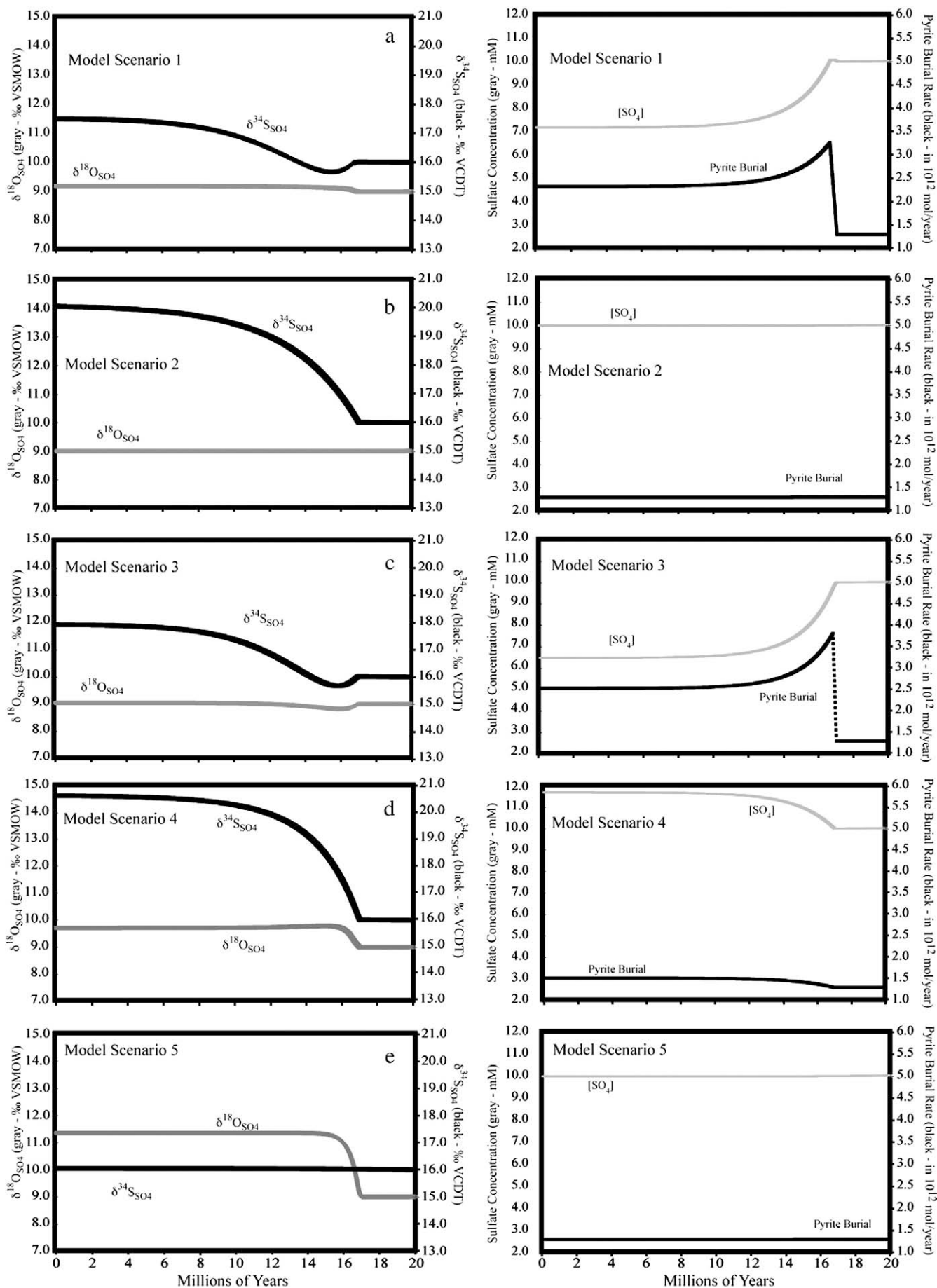
We first increase the flux of pyrite out of the ocean in model scenarios 1 and 3 (Fig. 5a, c). An increase in pyrite burial should increase the $\delta^{34}\text{S}_{\text{SO}_4}$ and decrease marine sulfate concentrations. We see that sulfate concentrations respond rapidly to the increased pyrite burial, decreasing by around 3 mM in both scenarios. In model scenario 1 (Fig. 5a), shelf area is doubled, causing an 80% increase in the pyrite burial flux. In model scenario 3 (Fig. 5c), we decrease the amount of sulfide reoxidized globally from 90% to 70%, causing a 95% increase in pyrite burial. The $\delta^{34}\text{S}_{\text{SO}_4}$ increases by 1.5‰ and 2‰ respectively and takes nearly 10 million years to reach its new steady state. The $\delta^{18}\text{O}_{\text{SO}_4}$ is affected by up to 0.5‰ from these changes in pyrite burial.

In model scenario 2 (Fig. 5b) we decrease the average $\delta^{34}\text{S}$ of pyrite by around 10‰. This could be caused by a change in microbial communities or sulfide scavenging efficiency that shifts the global average $\delta^{34}\text{S}$ of pyrite with out changing the net flux of sulfur out of the system. Another possibility is a decrease in the relative pyrite burial (to total sulfur burial), provided the total sulfur burial is unchanged. We assume that this change has no impact on the $\delta^{18}\text{O}_{\text{SO}_4}$. As shown in Fig. 5b, this decrease in the $\delta^{34}\text{S}$ of pyrite causes the $\delta^{34}\text{S}_{\text{SO}_4}$ to increase by 4‰ over 5 million years. Since we have not altered any of the fluxes in the sulfur cycle, there is no change to sulfate concentrations. Given the magnitude and rate of change in the $\delta^{34}\text{S}_{\text{SO}_4}$ in the Cretaceous, it is likely that some of this variability must be driven by changes in the $\delta^{34}\text{S}$ of pyrite, rather than solely by changes in the amount of pyrite buried, which has large consequences for marine sulfate concentrations. Unfortunately, confirming this hypothesis with measurements of the average $\delta^{34}\text{S}$ of pyrite could be extremely difficult; pyrite is a diagenetic mineral that grows from a constantly evolving $\delta^{34}\text{S}$ pool and even single crystals can have large isotope variations (Canfield and Teske, 1996).

In the fourth model scenario (Fig. 5d) we increase the river input as well as both the sulfur and oxygen isotopic composition of the river input; this simulates a shift to weathering evaporite minerals, which both erode more easily and are isotopically heavier. This change has a dramatic effect on the $\delta^{34}\text{S}_{\text{SO}_4}$ but a lesser effect on the $\delta^{18}\text{O}_{\text{SO}_4}$. It also causes an increase in marine sulfate concentrations of 2 mM and a concomitant increase in pyrite burial. The fact that the $\delta^{34}\text{S}_{\text{SO}_4}$ responds so dramatically to a shift in weathering suggests that changes in riverine input could be driving some of the changes seen in the marine $\delta^{34}\text{S}_{\text{SO}_4}$, but this should be accompanied by shifts in $\delta^{18}\text{O}_{\text{SO}_4}$ and would change marine sulfate concentration. This model scenario also demonstrates how much faster the $\delta^{18}\text{O}_{\text{SO}_4}$ responds to variations in fluxes in the sulfur cycle compared to the $\delta^{34}\text{S}_{\text{SO}_4}$ because of the different residence times. We feel these types of weathering changes, although they cannot be fully dismissed, are unlikely to be the primary driver of Cretaceous sulfur cycle variability because they should cause larger isotopic effects in the $\delta^{34}\text{S}_{\text{SO}_4}$ than in the $\delta^{18}\text{O}_{\text{SO}_4}$. Our record suggests the $\delta^{18}\text{O}_{\text{SO}_4}$ exhibits far larger shifts than the $\delta^{34}\text{S}_{\text{SO}_4}$ in the middle Cretaceous (Fig. 1).

The final model scenario (Fig. 5e) is included to demonstrate the impact of changing the sulfide oxidation pathway on marine $\delta^{18}\text{O}_{\text{SO}_4}$. The $\delta^{34}\text{S}_{\text{SO}_4}$ is not impacted because sulfur cycling in sediments is near-quantitative with little net fractionation is expressed. Because the net fluxes in and out of the ocean are not changed (nor is their sulfur isotope composition) in this model scenario, there is no change in either sulfate concentrations, pyrite burial, or $\delta^{34}\text{S}_{\text{SO}_4}$. This confirms our conclusion that the shifts in the $\delta^{18}\text{O}_{\text{SO}_4}$ in the Cretaceous are due to changes in the sulfide reoxidation pathway.

Fig. 5. Model results for the five model scenario runs summarized in the text. The $\delta^{18}\text{O}_{\text{SO}_4}$ and $\delta^{34}\text{S}$ are plot on the left and sulfate concentrations and pyrite burial rates are on the right. Model parameter changes are summarized in Table 1.



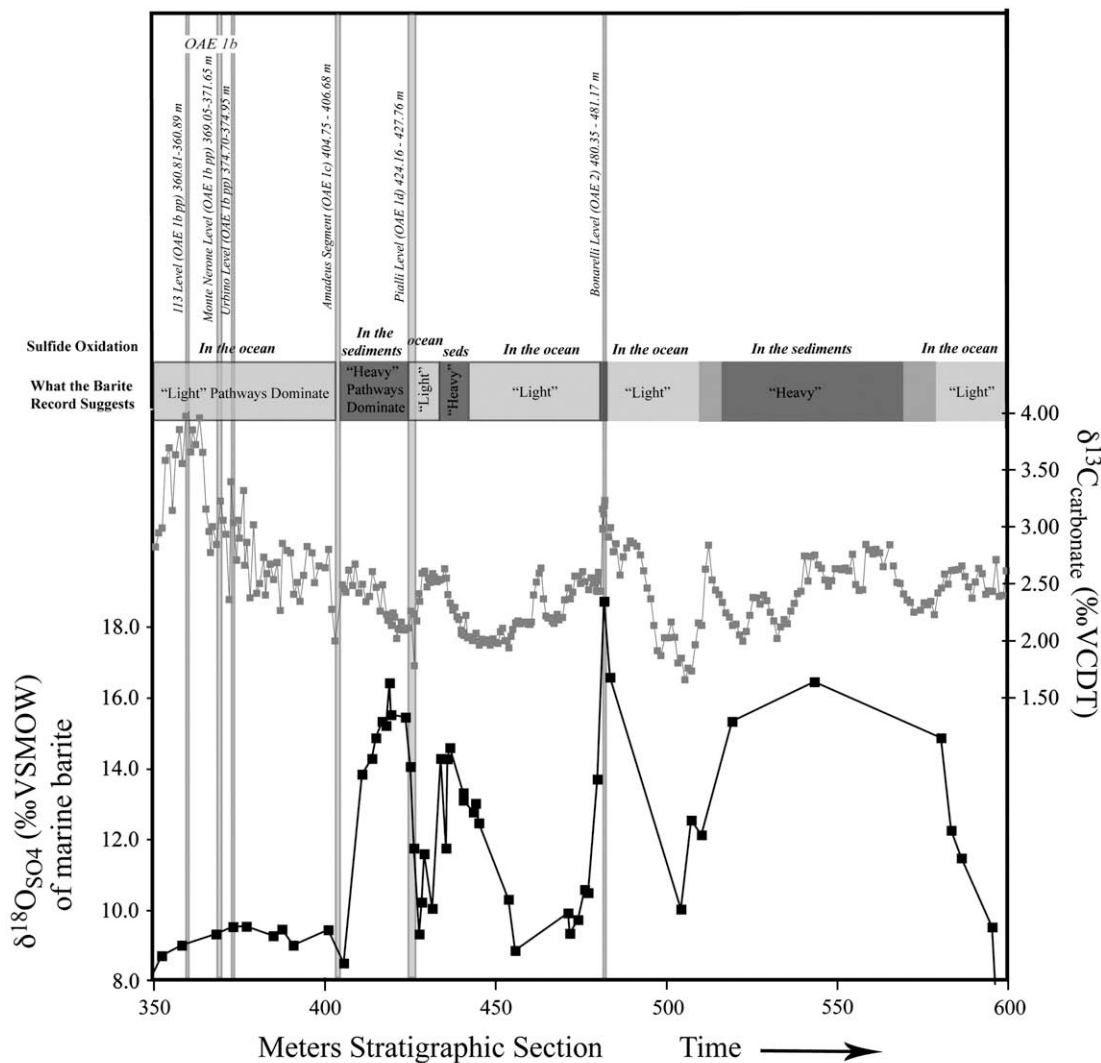


Fig. 6. Interpretive curve of the $\delta^{18}\text{O}_{\text{SO}_4}$ record with the $\delta^{13}\text{C}$ record to understand changes in the sulfur cycle over the Cretaceous.

What are driving the changes in the sulfide oxidation pathway and how are they coupled if at all to changes in the carbon cycle? In Fig. 6 we plot the $\delta^{18}\text{O}_{\text{SO}_4}$ along with the $\delta^{13}\text{C}$ of carbonate, which we use to highlight the timing of OAEs. Our interpretation is that when the $\delta^{18}\text{O}_{\text{SO}_4}$ increases then oxidation of sulfide is occurring dominantly in high organic-matter sediments under sub-oxic waters where microbial sulfide oxidizers proliferate. When the $\delta^{18}\text{O}_{\text{SO}_4}$ is much lower it is possible that the majority of sulfide oxidation occurs in the water column, suggesting that either organic carbon burial has become much more diffuse or the ocean has become euxinic and sulfide is freely available. It should be noted that this interpretation cannot distinguish between sulfide oxidation in the photic zone versus sulfide oxidation right above the sediment-water interface.

This interpretation raises several questions. First, does our data require periods of open ocean euxinia (that is “Black Sea” oceans) that may have persisted for millions of years? Our results are more nuanced and we are unable to make this conclusion. A shift from an ocean that has a $\delta^{18}\text{O}_{\text{SO}_4}$ of 9‰ to an ocean that has a $\delta^{18}\text{O}_{\text{SO}_4}$ of 16‰ requires a shift in the oxygen isotope fractionation during sulfide oxidation from 5–6‰ to 18–20‰; this is equivalent to a shift from an ocean where 60% of sulfide oxidation take places in diffuse organic carbon sediments or euxinic conditions to an ocean where nearly 100% of sulfide oxidation is microbially driven in sub-oxic waters (Turchyn

and Schrag, 2006). Are the former oceans in this scenario “euxinic”? Or does it represent sulfide oxidation in one ocean basin in the Cretaceous that has moved into the water column creating a globally large flux of isotopically lighter sulfate (e.g. Leckie et al., 2002). In the Cretaceous there were many more large, potentially restricted ocean basins (including the smaller North Atlantic, South Atlantic (relative to present), North west Tethys, and several epicontinental seas in Siberia and North America) where transient euxinia could have developed. But our data do not necessarily require that this condition also existed in the larger Pacific Ocean.

What our $\delta^{18}\text{O}_{\text{SO}_4}$ data do require is that there must have been rapid and dramatic changes in the sulfide oxidation pathway in the Cretaceous. Whether our measured shifts to lighter $\delta^{18}\text{O}_{\text{SO}_4}$ represent open water euxinia versus diffuse organic carbon burial could be tested using other euxinic-sensitive proxies, such as molybdenum isotopes or iron speciation in sediments.

5. Conclusions

We measured the $\delta^{34}\text{S}_{\text{SO}_4}$ and $\delta^{18}\text{O}_{\text{SO}_4}$ of coexisting barite and CAS from pelagic rocks through the middle Cretaceous. The $\delta^{18}\text{O}_{\text{SO}_4}$ of barite, unlike the $\delta^{34}\text{S}$ of barite, exhibited dramatic isotope shifts, which are temporally coincident with Ocean Anoxic Events. The

decoupling of the $\delta^{18}\text{O}_{\text{SO}_4}$ and the $\delta^{34}\text{S}_{\text{SO}_4}$ requires that the changes in the $\delta^{18}\text{O}_{\text{SO}_4}$ are driven by changes in the relative importance of the various sulfide oxidation pathways. Model results suggested that the likely driver of changes in the $\delta^{34}\text{S}_{\text{SO}_4}$ was changes in the isotopic composition of pyrite buried. After considering possible causes of the positive and negative oscillations in the $\delta^{18}\text{O}_{\text{SO}_4}$ we concluded that they could represent shifts to euxinia in some ocean basins during the middle Cretaceous. Using both sulfur and oxygen isotope data allowed a more complete understanding of the paleoceanographic sulfur cycle across this interval.

The $\delta^{34}\text{S}$ of the barite tracks the previously published $\delta^{34}\text{S}$ curve from Paytan et al. (2004) but the $\delta^{34}\text{S}$ of the CAS is isotopically different from the barite. The $\delta^{18}\text{O}_{\text{SO}_4}$ of coexisting barite and CAS are also isotopically distinct. We concluded that it was unlikely that the barite had been diagenetically altered. Rather, the difference in the isotopic composition of barite and CAS likely reflects a degradation of the CAS signal from carbonate recrystallization in pelagic sediments in the presence of isotopically altered pore fluid sulfate or possible contamination during the CAS extraction procedure.

Acknowledgements

We thank M. Hurtgen for discussions and technical assistance in developing our ability to extract and measure CAS. We thank G. Eischeid and F. Moore for laboratory assistance. This is publication no. 29 of the Centro di Geobiologia of the Urbino University. Reviews by D. Fike, W. Gilhooly, Y. Shen, T. Lyons, and one anonymous reviewer greatly improved this manuscript. This work was supported by Miller Institute for Basic Research, Schlanger Ocean Drilling Fellowship (AVT) Canadian Institute for Advanced Research (AVT and DPS), NSF Grant OCE-0452329 (DPS) and the Merck fund of the NY Community Trust (DPS).

Appendix A. Supplementary data

Supplementary data associated with this article can be found, in the online version, at doi:10.1016/j.epsl.2009.06.002.

References

- Arthur, M.A., Fisher, A.G., 1977. Upper Cretaceous–Paleocene magnetic stratigraphy at Gubbio, Italy I. Lithostratigraphy and sedimentology. *GSA Bull.* 88, 367–371.
- Arthur, M.A., Dean, W.E., Schlanger, S.O., 1985. Variations in the global carbon cycle during the Cretaceous related to climate, volcanism, and changes in atmospheric CO_2 . In: Sundquist, E.T., Broecker, W.S. (Eds.), *The Carbon Cycle and Atmospheric CO_2 : Natural Variations Archaen to Present: Geophysical Monograph Series*, vol. 32, pp. 504–529.
- Arthur, M.A., Brumsack, H.J., Jenkyns, H.C., Schlanger, S.O., 1990. Stratigraphy, geochemistry and paleoceanography of organic carbon-rich Cretaceous sequences. In: Ginsberg, R.N., Beaudoin, B. (Eds.), *Cretaceous Resources, Events and Rhythms*. InKluwell Publishers, Norwell MA, pp. 75–119.
- Berner, R.A., 2004. A model for calcium, magnesium, and sulfate in seawater over Phanerozoic Time. *Am. J. Sci.* 304, 438–453.
- Bishop, J.K.W., 1988. The barite-opal-organic carbon association in oceanic particulate matter. *Nature* 332, 341–343.
- Brand, U., Veizer, J., 1980. Chemical diagenesis of a multicomponent carbonate system I. Trace elements. *J. Sediment. Petrol.* 50 (4), 1219–1236.
- Burdett, J.W., Arthur, M.A., Richardson, M., 1989. A Neogene seawater sulfate isotope age curve from calcareous pelagic microfossils. *Earth Planet. Sci. Lett.* 94, 189–198.
- Canfield, D.E., Teske, A., 1996. Late Proterozoic rise in atmospheric oxygen concentration inferred from phylogenetic and sulphur-isotope studies. *Nature* 382, 127–132.
- Claypool, G.E., Holser, W.T., Kaplan, I.R., Sakai, H., Zak, I., 1980. The age curves of sulfur and oxygen isotopes in marine sulfate and their mutual interpretation. *Chem. Geol.* 28, 199–260.
- Cocconi, R., 1996. The cretaceous of the Umbria-Marche Apennines (Central Italy). *J. Wiedmann Symposium, Cretaceous Stratigraphy, Paleobiology and Paleobiogeography*, pp. 129–136.
- Falkowski, P.G., Katz, M.E., Milligan, A.J., Fennel, K., Cramer, B.S., Aubry, M.P., Berner, R.A., Novacek, M.J., Zapol, W.M., 2005. The rise of oxygen over the past 205 million years and the evolution of large placental mammals. *Science* 309, 2202–2205.
- Fantle, M.S., DePaolo, D.J., 2007. Ca isotopes in carbonate sediment and pore fluid from ODP Site 807A: the Ca^{2+} (aq) – calcite equilibrium fractionation factor and calcite recrystallization rates in Pleistocene sediments. *Geochim. Cosmochim. Acta* 71, 2524–2547.
- Fike, D.A., Grotzinger, J.P., Pratt, L.M., Summons, R.E., 2006. Oxidation of the Ediacaran Ocean. *Nature* 444, 744–747.
- Ganeshram, R.S., Francois, R., Commeau, J., Brown-Leger, S.L., 2003. An experimental investigation of Barite formation in seawater. *Geochim. Cosmochim. Acta* 67 (14), 2599–2605.
- Gill, B.C., Lyons, T.W., Saltzman, M.R., 2007. Parallel, high-resolution carbon and sulfur isotope records of the evolving Paleozoic marine sulfur reservoir. *Palaeogeogr. Palaeoclimatol. Palaeoecol.* 256, 156–173.
- Gradstein, et al., 2004. *A Geologic Time Scale*. Cambridge Univ. Press, New York.
- Halverson, G.P., Dudas, F.O., Maloof, A.C., Bowring, S.A., 2007. Evolution of the $^{87}\text{Sr}/^{86}\text{Sr}$ composition of Neoproterozoic seawater. *Palaeogeogr. Palaeoclimatol. Palaeoecol.* 256, 103–129.
- Horita, J., Zimmermann, H., Holland, H.D., 2002. Chemical evolution of seawater during the Phanerozoic: implications from the record of marine evaporates. *Geochim. Cosmochim. Acta* 66, 3733–3756.
- Hurtgen, M.T., Arthur, M.A., Suits, N.S., Kaufman, A.J., 2002. The sulfur isotopic composition of Neoproterozoic seawater sulfate: implications for a snowball Earth? *Earth Planet. Sci. Lett.* 203, 413–429.
- Hurtgen, M.T., Halverson, G.P., Arthur, M.A., Hoffman, P.F., 2006. Sulfur cycling in the aftermath of a 635-Ma snowball glaciation: evidence for a syn-glacial sulfidic deep ocean. *Earth Planet. Sci. Lett.* 245, 551–570.
- Jenkyns, H.C., 1980. Ocean anoxic events: from the continents to the oceans. *J. Geol. Soc. Lond.* 137, 171–188.
- Kasten, S., Jørgensen, B.B., 2000. Sulfate reduction in marine sediments. In: Schulz, H.D., Zabel, M. (Eds.), *Marine Geochemistry*, pp. 263–275.
- Kampschulte, A., Strauss, H., 2004. The sulfur isotopic evolution of Phanerozoic seawater based on the analysis of structurally substituted sulfate in carbonates. *Chem. Geol.* 204, 255–286.
- Leckie, R.M., Bralower, T.J., Cashman, R., 2002. Oceanic anoxic events and plankton evolution: biotic response to tectonic forcing during the mid-Cretaceous. *Paleoceanography* 17 (3) Article No. 1029.
- Lloyd, R.M., 1968. Oxygen isotope behavior in the sulfate-water system. *J. Geophys. Res.* 73, 6099–6110.
- Lowenstein, T.K., Timofeeff, M.N., Brennan, S.T., Hardie, L.A., Demicco, R.V., 2001. Oscillations in Phanerozoic seawater chemistry: evidence from fluid inclusions. *Science* 294, 1086–1088.
- Ludden, J.N., Gradstein, F.M., and the Shipboard Scientific Party, 1990. *Proceedings of the Ocean Drilling Program, Initial Reports*, vol. 123. doi:10.2973/odp.proc.ir.123.105.1990.
- Lyons, T.W., Walter, L.M., Gellatly, A.M., Martini, A.M., Blake, R.E., 2004. Sites of anomalous organic remineralization in the carbonate sediments of South Florida, USA: the sulfur cycle and carbonate-associated sulfate. In: Amend, J.P., Edwards, K.J., Lyons, T.W. (Eds.), *Sulfur Biogeochemistry: Past and Present: Geological Society of America Special Paper*, vol. 379, pp. 161–176.
- Marenco, P.J., Corsetti, F.A., Hammond, D.E., Kaufman, A.J., Bottjer, D.J., 2008. Oxidation of pyrite during extraction of carbonate associated sulfate. *Chem. Geol.* 247, 124–132.
- Moberly, R., Gardner, J.V., Larson, R.L., and the Shipboard Scientific Party, 1975. *Proceedings of the Deep Sea Drilling Program Initial Reports*, vol. 32. doi:10.2973/dsdp.proc.32.104.1975.
- Morse, J.W., Mackenzie, F.T., 1990. *Geochemistry of Sedimentary Carbonates*. Elsevier, Amsterdam.
- Paytan, A., Kastner, M., Campbell, D., Thiemens, M.H., 1998. Sulfur isotopic composition of cenozoic seawater sulfate. *Science* 282, 1459–1463.
- Paytan, A., Mearon, S., Cobb, K., Kastner, M., 2002. Origin of marine barite deposits: Sr and S isotope characterization. *Geology* 30, 747–750.
- Paytan, A., Kastner, M., Campbell, D., Thiemens, M.H., 2004. Seawater Sulfur Isotope Fluctuations in the Cretaceous. *Science* 304, 1663–1665.
- Petsch, S.T., Berner, R.A., 1996. Coupling the geochemical cycles of C, P, Fe, and S: the effect on atmospheric O_2 and the isotopic records of carbon and sulfur. *Am. J. Sci.* 298, 246–262.
- Shields, G.A., Strauss, H., Howe, S.S., Siegmund, H., 1999. Sulphur isotope compositions of sedimentary phosphorites from the basal Cambrian of China: implications for Neoproterozoic-Cambrian biogeochemical cycling. *J. Geol. Soc. (Lond.)* 156, 943–955.
- Sprovieri, M., Cocconi, R., Lirer, F., Pelosi, N., Lozar, F., 2006. Orbital tuning of a lower Cretaceous composite record (Maiolica Formation, central Italy). *Paleoceanography* 21, PA4212. doi:10.1029/2005PA001224.
- Strauss, H., 1999. Geological evolution from isotope proxy signals – sulfur. *Chem. Geol.* 161, 89–101.
- Torres, M.E., Brumsack, H.J., Bohrmann, G., Emeis, K.C., 1996. Barite fronts in continental margin sediments: a new look at barium remobilization in the zone of sulfate reduction and formation of heavy barites in diagenetic fronts. *Chem. Geol.* 127, 125–139.
- Turchyn, A.V., Schrag, D.P., 2004. Oxygen isotope constraints on the sulfur cycle over the past 10 million years. *Science* 303, 2004–2007.
- Turchyn, A.V., Schrag, D.P., 2006. Cenozoic evolution of the sulfur cycle: insight from oxygen isotopes in marine sulfate. *Earth Planet. Sci. Lett.* 241, 763–779.
- Van Stempvoort, D.R., Krouse, H.R., 1994. Controls of $\delta^{18}\text{O}$ in sulfate: review of experimental data and application to specific environments. *Environmental Geochemistry of Sulfide Oxidation*. American Chemical Society, pp. 446–480.
- Walter, L.M., Ku, T.C.W., Muehlenbachs, K., Patterson, W.P., Bonnell, L., 2007. Controls on the $\delta^{13}\text{C}$ of dissolved inorganic carbon in marine pore waters: an integrated case study of isotope exchange during syndepositional recrystallization of biogenic carbonate sediments (South Florida Platform, USA). *Deep Sea Res. II* 54, 1163–1200.
- Wortmann, U.G., Chernyavsky, B., Bernasconi, S.M., Brunner, B., Böttcher, M.E., Swart, P.K., 2007. Oxygen isotope biogeochemistry of pore water sulfate in the deep biosphere: dominance of isotope exchange reactions with ambient water during microbial sulfate reduction (ODP Site 1130). *Geochim. Cosmochim. Acta* 71 (17), 4221–4232.